Journal of the Mechanics and Physics of Solids 60 (2012) 1644–1659

Contents lists available at SciVerse ScienceDirect

Journal of the Mechanics and Physics of Solids

journal homepage: www.elsevier.com/locate/jmps

Theory of sorption hysteresis in nanoporous solids: Part I Snap-through instabilities

Zdeněk P. Bažant [a,*], Martin Z. Bazant [b]

[a] McCormick School, Civil Engineering and Materials Science, Northwestern University, 2145 Sheridan Road, CEE/A135, Evanston, IL 60208, United States
[b] Chemical Engineering and Mathematics, Massachusetts Institute of Technology, Cambridge, MA 02139, United States

ARTICLE INFO

Article history:
Received 26 October 2011
Received in revised form
23 April 2012
Accepted 29 April 2012
Available online 9 May 2012

Keywords:
Hindered adsorption
Disjoining pressure
Diffusion of water
Drying of concrete
Internal surface

ABSTRACT

The sorption–desorption hysteresis observed in many nanoporous solids, at vapor pressures low enough for the liquid (capillary) phase of the adsorbate to be absent, has long been vaguely attributed to some sort of 'pore collapse'. However, the pore collapse has never been documented experimentally and explained mathematically. The present work takes an analytical approach to account for discrete molecular forces in the nanopore fluid and proposes two related mechanisms that can explain the hysteresis at low vapor pressure without assuming any pore collapse nor partial damage to the nanopore structure. The first mechanism, presented in Part I, consists of a series of snap-through instabilities during the filling or emptying of non-uniform nanopores or nanoscale asperities. The instabilities are caused by non-uniqueness in the misfit disjoining pressures engendered by a difference between the nanopore width and an integer multiple of the thickness of a monomolecular adsorption layer. The wider the pore, the weaker the mechanism, and it ceases to operate for pores wider than about 3 nm. The second mechanism, presented in Part II, consists of molecular coalescence, or capillary condensation, within a partially filled surface, nanopore or nanopore network. This general thermodynamic instability is driven by attractive intermolecular forces within the adsorbate and forms the basis for developing a unified theory of both mechanisms. The ultimate goals of the theory are to predict the fluid transport in nanoporous solids from microscopic first principles, determine the pore size distribution and internal surface area from sorption tests, and provide a way to calculate the disjoining pressures in filled nanopores, which play an important role in the theory of creep and shrinkage.

1. Introduction

The sorption isotherm, characterizing the isothermal dependence of the adsorbate mass content on the relative vapor pressure at thermodynamic equilibrium, is a basic characteristic of adsorbent porous solids. It is important for estimating the internal pore surface of hydrated Portland cement paste and other materials. It represents the essential input for solutions of the diffusion equation for drying and wetting of concrete, for calculations of the release of methane from coal deposits and rock masses, for the analysis of sequestration of carbon dioxide in rock formations, etc. Its measurements

* Corresponding author. Tel.: +1 847 491 4025; fax: +1 847 491 4011.
E-mail address: z-bazant@northwestern.edu (Z.P. Bažant).

0022-5096/$ - see front matter © 2012 Published by Elsevier Ltd.
http://dx.doi.org/10.1016/j.jmps.2012.04.014

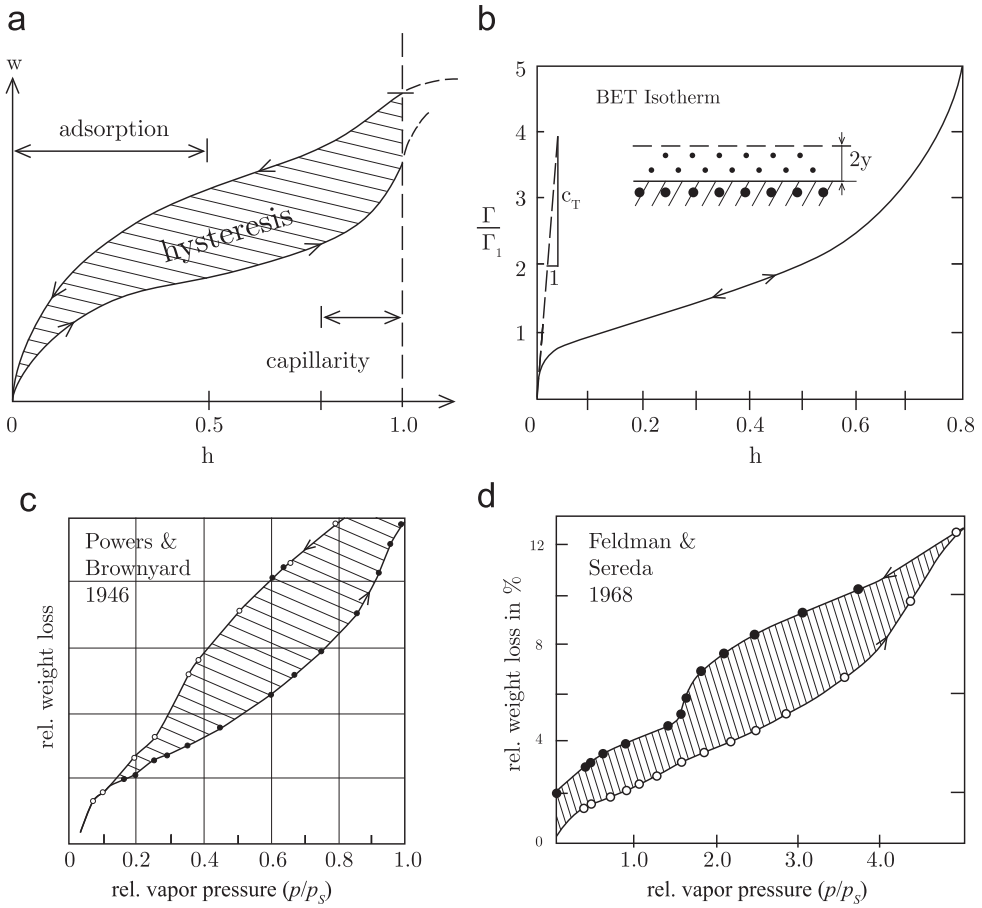

Fig. 1. (a) Typical desorption and sorption isotherms; (b) BET isotherm; (c) and (d) desorption and sorption isotherms measured on hardened Portland cement paste.

provide vital information for determining the internal surface of nanoporous solids (Powers and Brownyard, 1946; Adolphs and Setzer, 1996; Jennings, 2000; Adolphs et al., 2002; Espinosa and Franke, 2006; Baroghel-Bouny, 2007).

An important feature of sorption experiments with water, nitrogen, alcohol, methane, carbon dioxide, etc. has been a pronounced hysteresis, observed at both high and low vapor pressures and illustrated by two classical experiments in Fig. 1c and d; in Powers and Brownyard (1946, p. 277) and Feldman and Sereda (1964) (see also, e.g. Feldman and Sereda, 1968; Rarick et al., 1995; Adolphs et al., 2002; Espinosa and Franke, 2006; Baroghel-Bouny, 2007). For adsorbates that exist at room temperature in a liquid form, e.g. water, the room temperature hysteresis at high vapor pressures near saturation has easily been explained by non-uniqueness of the surfaces of capillary menisci of liquid adsorbate in larger pores (e.g., the 'ink-bottle' effect Brunauer, 1943).

However, a liquid (capillary) water can exist in the pores only if the capillary tension under the meniscus (which is given by the Kelvin–Laplace equation) does not exceed the tensile strength of liquid water, which is often thought to be exhausted at no less than 45% of the saturation pressure, if not much higher. Anyway, at vapor pressures less than about 80% of the saturation pressure, the liquid phase represents a small fraction of the total evaporable water content of calcium silicate hydrates (C–S–H) (Jennings, submitted for publication); see Fig. 1a.

For more than 60 years, the hysteresis in the range of low vapor pressures (lower than about 80% of saturation in the case of C–S–H) has remained a perplexing and unexplained feature. In that range, most or all of the adsorbate is held by surface adsorption. The gases and porous solids of interest generally form adsorption layers consisting of several monomolecular layers (Fig. 1b). The multi-layer adsorption is described by the BET isotherm (Brunauer et al., 1938) (Fig. 1b), which is reversible. Sorption experiments have generally been interpreted under the (tacit) hypothesis of free adsorption, i.e., the adsorption in which the surface of the adsorption layer is exposed to gas.

In nanoporous solids, though, most of the adsorbate is in the form of hindered adsorption layers, i.e., layers confined in the nanopores which are sometimes defined as pores ≤ 2 nm wide (Balbuena et al., 1993). For instance, 1 cm^3 of hardened Portland cement paste contains the internal surface of about 500 m^2. The total porosity is typically about 50%, with the large capillary pores occupying about 15% and the nanopores about 35% of the material volume. So, the average width of nanopores is about 0.35 $cm^3/500\ m^2 = 0.7$ nm, which is about three water molecular diameters. The hindered adsorbed layers in such nanopores have no surface directly exposed to vapor and communicate with the vapor in macropores by diffusion along the layer. It has been well known that a large transverse stress, called the disjoining pressure (Derjaguin, 1940) (or solvation pressure Balbuena et al., 1993), must develop in these layers.

Development of the theory of hindered adsorption for concrete was stimulated by Powers' general ideas of the creep mechanism (Powers, 1966). Its mathematical formulation for C–S–H gradually emerged in Bažant (1970a, 1970b, 1972a, 1972b), and was reviewed in a broad context in Bažant (1975). But this theory of hindered adsorption is also reversible. Thus, although a theory exists, it cannot explain the hysteresis.

The sorption hysteresis in hardened Portland cement paste, concrete and various solid gels (Scherer, 1999; Jennings et al., 2008) has for decades been vaguely attributed to some sort of changes of the nanopore structure. In particular, it was proposed that the exit of water, called the interlayer water, from the narrowest nanopores would somehow cause the pores to collapse (Feldman and Sereda, 1968; Espinosa and Franke, 2006; Baroghel-Bouny, 2007; Thomas et al., 2008) (see Rarick et al., 1995, Figs. 13 and 16, Espinosa and Franke, 2006, Fig. 1, or Jennings, submitted for publication, Fig. 9), picturing hypothesized pore width changes of the order of 100%.

However, if a mathematical model of such a mechanism is attempted, it inevitably predicts enormous macroscopic deformations, far larger than the observed shrinkage caused by drying. For example, measurements on the hardened cement paste reveal desorption and sorption isotherms (Fig. 1) in which the water contents w for the same humidity h differ by 50% or more. As before, consider that the nanopores represent 35% of the total volume of material. Thus, if the 50% difference in w were totally due to collapsing nanopores, the relative volume change in the material would have to be about $0.35\times 0.50=0.175$. This means that the pore collapse would have to cause a linear shrinkage of about $0.175/3\approx 6\%$. But the typical drying shrinkage of hardened cement pastes is one to two orders-of-magnitude smaller. Although the results of a more accurate analysis could differ by a factor of up to about 2, there is no way the hypothesis of pore collapse could be quantitatively reconciled with the shrinkage observations.

Another objection to the pore collapse hypothesis is that the isotherm for second desorption is much closer to that for first desorption than to that for first sorption. If this hypothesis was true, then the pores would have to get somehow reconstructed prior to the second desorption. So, the pore collapse hypothesis is untenable (and so is the use of this hypothesis for explaining the increase in creep of concrete due to simultaneous drying: Feldman and Sereda, 1968).

Another idea, qualitatively inferred from environmental scanning electron microscope studies (Hall et al., 1995), was to explain the hysteresis in cement pastes by new hydration of unreacted remnants of cement grains and the associated swelling which would be encroaching into the pore space and also causing pore wall damage. But how could one then explain that the second desorption isotherm is close to the first (Powers and Brownyard, 1946; Baroghel-Bouny, 2007)? Surely one cannot expect the grains to reversibly dehydrate during wetting sorption, and the pore wall damage to get repaired. Besides, in bulk, no measurable cement hydration takes place at pore humidities below about 0.70–0.85.

Here it will be shown that sorption hysteresis must occur even if the nanopore structure does not change. The main message of this work is that the number of molecular layers of adsorbate that can be confined in a nanopore is not unique, and that this non-uniqueness inevitably causes sorption hysteresis.

Non-uniqueness is also a salient feature of capillarity of liquid water in larger pores, typically of micrometer dimensions. In the capillary range, the non-uniqueness is classically explained by the afore-mentioned 'ink-bottle' effect, which exists even in two dimensions. In three dimensions, there is much broader range of topological and geometrical configurations which provide a richer and more potent source of non-uniqueness of liquid adsorbate content.

The simplest demonstration is a regular cubic array of identical spherical particles separated by a small gap δ between each pair. At $h=1$, either all the pore space can be filled by a liquid, or an anticlastic meniscus surface of a zero total curvature $r^{-1}=r_1^{-1}+r_2^{-1}=0$ and of a liquid pressure equal to p_s can exist between each two spheres, with $r_1=-r_2$ and $r_1,r_2=$ principal curvature radii (the surface near the symmetry line of the pair of spheres is a rotational hyperbolic paraboloid). Such effects can explain 100% differences among equilibrium liquid contents w at $h=1$ observed in some experiments. It can even be shown that when both δ and r_1 (with $r_2=-r_1$) approach zero in a certain way, then also the liquid content (as a continuum) approaches 0 (thus, in theory, an arbitrarily small but non-zero equilibrium liquid content at $h=1$ is possible, though extremely unlikely).

This three-dimensional picture, for example, explains why the non-uniqueness of sorption isotherm extends to $h>1$ (as shown in Fig. 1a by dashed lines); here $h=p_v/p_s(T)$ is the relative vapor pressure, or relative humidity in the case of water, p_v is the pressure of vapor or gas; and $p_s(T)$ is the saturation vapor pressure). For $h>1$, the vapor pressure $p_v>p_s$, the total curvature of the menisci is changed from positive to negative, the pores contain overpressurized vapor, and the hysteresis, or non-uniqueness, continues (Bažant and Thonguthai, 1978; Bažant and Kaplan, 1996). This non-uniqueness and hysteresis explains why the slope of the isotherm for $h>1$ is one, or even two, orders of magnitude higher than one would calculate if all the water were liquid for $h>1$ (in theory, this non-uniqueness can extend up to the critical point of water). In cements these phenomena are complicated by the fact that the chemical reactions of hydration withdraw some water from the pores, and create self-desiccation bubbles (thus one can practically never have concrete with no vapor, even for $p_v>p_s$).

The consequence of the non-uniqueness is that the sorption isotherm is not a function but a functional of the entire previous history of adsorbate content. Here we will show that the functional character extends to the range of hindered adsorption in nanopores.

The recent advent of molecular dynamic (MD) simulations is advancing the knowledge of nanoporous solids and gels or colloidal systems in a profound way (Pellenq et al., 2010; Coasne et al., 2008a, 2008b, 2009; Jönson et al., 2004, 2005; Smith et al., 2006; Malani et al., 2009; Vandamme et al., 2010). Particularly exciting have been the new results by Rolland Pellenq and co-workers at the Concrete Sustainability Hub (CSH) in MIT led by Franz-Josef Ulm (Bonnaud et al., 2010;

Brochard et al., 2011, 2012). These researchers used numerical MD simulations to study sorption and desorption in nanopores of coal and calcium silicate hydrates. Their MD simulations (Bonnaud et al., 2010, Figs. 3 and 4) demonstrated that the filling and emptying of pores 1 and 2 nm wide by water molecules exhibits marked hysteresis.

Especially revealing is the latest article of Pellenq et al. from MIT (Brochard et al., 2011). Simulating a chain of nanopores, they computed the distributions of disjoining (or transverse) pressure and found that it can alternate between negative (compressive) and positive (tensile), depending on the difference of pore width from an integer multiple of the natural thickness of an adsorbed monomolecular layer (see Brochard et al., 2011, Figs. 14 and 11). This discrete aspect of disjoining pressure, which cannot be captured by continuum thermodynamics, was a crucial finding of Pellenq et al. which stimulated the mathematical formulation of snap-through instabilities in Part I of this work. Oscillations between positive and negative disjoining pressures have also been revealed by density functional theory simulations of colloidal fluids or gels in Balbuena et al. (1993) (where the excess transverse stress is called the 'solvation pressure' rather than the disjoining pressure).

Nanoscale oscillations of the disjoining (or solvation) pressure have also been observed in the MD simulations of nitrogen molecules in rough slit-shaped carbon nanopores (using for carbon the quenched solid density functional theory) (Yang et al., 2011). It was concluded that the surface roughness damps these oscillations. This phenomenon may be important for the meso- or macroscale residual stresses and creep in C–S–H but, as argued here, not for the sorption isotherms that are dominated by dynamic snap-throughs.

This work is organized as follows. In Part I, we begin by summarizing the classical theory of multi-layer adsorption on free surfaces by Brunauer, Emmett and Teller (BET) (Brunauer et al., 1938), which is widely used to fit experimental data, but assumes reversible adsorption without any hysteresis. We then develop a general theory of hindered adsorption in nanopores which accounts for crucial and previously neglected effects of molecular discreteness as the pore width varies. This leads us to the first general mechanism for sorption hysteresis, snap-through instability in non-uniform pores, which is the focus of this Part I.

In Part II which follows (Bazant and Bažant), we show that the attractive forces between discrete adsorbed molecules can also lead to sorption hysteresis by molecular condensation in arbitrary nanopore geometries, including perfectly flat surfaces and pores. This second mechanism of hysteresis is a general thermodynamic instability of the homogeneous adsorbate that leads to stable high-density and low-density phases below the critical temperature. The mathematical formulation of Part II is thus based on non-equilibrium statistical mechanics. But here, in Part I, we begin to build the theory using more familiar models from solid mechanics and continuum thermodynamics.

2. Continuum thermodynamics of hindered adsorption in nanopores

Free adsorption: When a multi-molecular adsorption layer on a solid adsorbent surface is in contact with the gaseous phase of the adsorbate, the effective thickness a of the layer is well described by the BET equation (Brunauer et al., 1938, Eq. (28))

$$\Theta = \frac{a}{s_0} = \frac{\Gamma_w}{\Gamma_1} = \frac{1}{1-h} - \frac{1}{1-h+c_T h}, \quad c_T = c_0 e^{\Delta Q_a/RT} \tag{1}$$

where T is the absolute temperature, Γ_w is the mass of adsorbate per unit surface area; Γ_1 is the mass of one full molecular monolayer per unit area, Θ is the dimensionless surface coverage, h is the relative pressure of the vapor in macropores with which the adsorbed water is in thermodynamic equilibrium, R is the universal gas constant (8314 J kmole^{-1} K^{-1}), c_0 is the constant depending on the entropy of adsorption, ΔQ_a is the latent heat of adsorption minus latent heat of liquefaction, s_0 is the effective thickness of a monomolecular layer of the adsorbate, a is the effective thickness of the free adsorption layer in contact with vapor (Fig. 1b), which attains saturation at the maximum thickness of about five monolayers.

Powers (1965), using the BET isotherm, estimated in 1965 that a monomolecular water adsorption layer in cement paste was complete at $h=12\%$ and a bimolecular one at 51%. This would imply that $c_T \approx 54$, which is the value used in the plot of BET isotherm in Fig. 1b. However, because of the new phenomena discussed here and in Part II which follows (Bazant and Bažant), this estimate of c_T is likely to be far too high.

Eq. (1) can be easily inverted

$$h = h(a) = A + \sqrt{A^2 + B} \tag{2}$$

where

$$A = \frac{Bc_T}{2}\left(1 - \frac{s_0}{a}\right), \quad B = \frac{1}{c_T - 1} \tag{3}$$

Hindered adsorption: Consider now a pore with planar rigid adsorbent walls parallel to the coordinates x and z, and a width $2y$ that is smaller than the combined width $2a$ of the free adsorption layers at the opposite walls given by Eq. (1). Then, the adsorbate has no surface in contact with the vapor and full free adsorption layers are prevented from building up at the opposite pore walls, i.e., the adsorption is hindered and a transverse pressure, p_d, called the disjoining pressure (Derjaguin, 1940), must develop. For water in C–S–H, which is highly hydrophillic, the adsorption layers can be up to 5

molecules thick, and so hindered adsorption can exist only in pores less than 10 molecules wide ($2y < 2.6$ nm). Here in Part I we deal solely with pores of such width. The hindered adsorption with disjoining pressure will develop when h is high enough to fill the pore. The hindered adsorbate communicates by diffusion along the pore with the vapor in an adjacent macropore.

In a process in which thermodynamic equilibrium is maintained, the chemical potentials μ of the vapor and its adsorbate, representing the Gibbs' free energy per unit mass, must remain equal. So, under isothermal conditions

$$\mathrm{d}\mu = \rho_a^{-1}(\mathrm{d}\tilde{p}_d + 2\mathrm{d}p_a)/3 = \rho_v^{-1}\,\mathrm{d}p_v \tag{4}$$

here ρ is the mass density of the vapor and ρ_a is the average mass density of the adsorbate (which probably is, in the case of water, somewhere between the mass density ρ_w of liquid water and ice). The superscript ˜ is attached to distinguish the disjoining pressure obtained by continuum analysis from that obtained later by discrete molecular considerations ($\tilde{p}_d = 0$ if the nanopore is not filled because the transverse pressure due to water vapor is negligible); $p_a = \pi_a/y$ is the in-plane pressure in the adsorption layer averaged through the thickness of the hindered adsorption layer; it has the dimension of N/m^2, and (in contrast to stress) is taken positive for compression; π_a is the longitudinal spreading 'pressure' in the adsorption half-layer of thickness y (here the term 'pressure' is a historically rooted misnomer; its dimension is not pressure, N/m^2, but force per unit length, N/m); π_a is superposed on the solid surface tension $g a_s$, which is generally larger in magnitude, and so the total surface tension, $\gamma = \gamma_s - p_a$, is actually tensile (see Bažant, 1972a, Fig. 2) (thus the decrease in spreading pressure with decreasing h causes an increase in surface tension, which is one of the causes of shrinkage).

Further note that if p_d and p_a were equal, the left-hand side would be $\mathrm{d}\mu = \rho_a^{-1}\,\mathrm{d}p_d$, which is the standard form for a bulk fluid. Also, in contrast to solid mechanics, the left-hand side of Eq. (4) cannot be written as $\epsilon_y\,\mathrm{d}p_d + 2\epsilon_x\,\mathrm{d}p_a$ because strains ϵ_x and ϵ_y cannot be defined (since the molecules in adsorption layers migrate and the difference between p_d and p_a is caused by the forces from solid adsorbent wall rather than by strains).

Consider now that the ideal gas equation $p_v \rho_v^{-1} = RT/M$ applies to the vapor (M=molecular weight of the adsorbate; e.g., for water M=18.02 kg/kmole). Upon substitution into Eq. (4), we have the differential equation

$$\text{for } h \le h_f: \quad \rho_a^{-1}\,\mathrm{d}p_a = (RT/M)\,\mathrm{d}p_v/p_v \tag{5}$$

$$\text{for } h > h_f: \quad \rho_a^{-1}(\mathrm{d}\tilde{p}_d + 2\,\mathrm{d}p_a)/3 = (RT/M)\,\mathrm{d}p_v/p_v \tag{6}$$

where h_f is the value of h at which the nanopore of width $2y$ gets filled, i.e., $h_f = h(y)$ based on Eq. (2). Factors 2 and 3 do not appear for $h < h_f$ because the free adsorbed layer can expand freely in the thickness direction. Integration of Eq. (4) under the assumption of constant ρ_a yields

$$\text{for } h \le h_f: \quad p_a = \frac{\pi_a}{y} = \rho_a \frac{RT}{M} \ln h \tag{7}$$

$$\text{for } h > h_f: \quad \tilde{p}_d + 2(p_a - p_{af}) = 3\rho_a \frac{RT}{M} \ln \frac{h}{h_f} \tag{8}$$

where $p_{af} = p_a(h_f)$ is the longitudinal pressure when the nanopore just gets filled, i.e., when $a = y$.

It is now convenient to introduce the ratio of the increments of in-plane and disjoining pressures

$$\kappa = \mathrm{d}p_a/\mathrm{d}\tilde{p}_d \tag{9}$$

which we will call the disjoining ratio. If the adsorbate was a fluid, κ would equal to 1. Since it is not, $\kappa \neq 1$. The role of κ is analogous to the Poisson ratio of elastic solids. A rigorous calculation of κ would require introducing (aside from surface forces) the constitutive equation relating p_a and p_d (this was done in Bažant and Moschovidis (1973), but led to a complex hypothetical model with too many unknown parameters).

We will consider κ as constant, partly for the sake of simplicity, partly because (as clarified later) κ is determined by inclined forces between the pairs of adsorbate molecules (Fig. 3b and c); κ should be constant in multi-molecular layers because the orientation distribution of these forces is probably independent of the nanopore width. Note that κ would be equal to 0 only if all these intermolecular forces were either in-plane or orthogonal (as in a rectangular grid, Fig. 3a).

For constant disjoining ratio κ, we may substitute $p_a = \kappa \tilde{p}_d$ in Eq. (8), and we get

$$\tilde{p}_d = \frac{\rho_a}{1+2\kappa} \frac{RT}{M} \ln \frac{h}{h_f} \tag{10}$$

For $\kappa = 0$, this equation coincides with Eq. (29) in Bažant (1972a) but, in view of Fig. 3, a zero κ must be an oversimplification.

According to this continuum model of hindered adsorption, which represents a minor extension of Bažant (1972a), the sorption isotherm of the adsorbate mass as a function of vapor pressure would have to be reversible. However, many classical and recent experiments (Powers and Brownyard, 1946; Feldman and Sereda, 1964; Rarick et al., 1995; Espinosa and Franke, 2006; Baroghel-Bouny, 2007) as well as recent molecular simulations (Bonnaud et al., 2010; Brochard et al., 2011, 2012) show it is not. Two mutually related mechanisms that must cause sorption irreversibility in nanopores with fixed rigid walls will be presented, one here in Part I, and one in Part II which follows (Bazant and Bažant).

3. Mechanism I: snap-through instability

The local transverse (or disjoining) pressure p_d can be determined from the transverse stiffness C_n, defined as $C_n = \Delta F/\Delta s$, where ΔF is the transverse resisting force per molecule and Δs is the change of spacing (or distance) between the adjacent monomolecular layers in a nanopore containing n monomolecular layers of the adsorbate. Since large changes of molecular separation are considered, C_n varies with s and should be interpreted as the secant modulus in the force–displacement diagram (Fig. 2b). For this reason, and also because many bond forces are inclined ('lateral interactions' (Nikitas, 1996; Cerofolini and Meda, 1998a, 1998b)) rather than orthogonal with respect to the adsorption layer (shown by the bars in Fig. 3), C_n is generally the same as neither the second derivative $d^2\Phi/dr^2$ of interatomic potential nor the first derivative dF/ds of force F (Fig. 2a and b).

To estimate C_n, one could consider various idealized arrangements of the adsorbate molecules (as depicted two-dimensionally for two different pore widths $2y$ in Fig. 3) and thus obtain analytical expressions for C_n based on the classical mechanics of statically indeterminate elastic trusses. However, in view of all the approximations and idealizations, it makes no sense to delve into these details.

Diverging nanopore: Consider now a wedge-shaped nanopore between two diverging planar walls of the adsorbent (Fig. 4a), having the width of $2y$, where $y = kx$. Here x is the longitudinal coordinate (Fig. 4), k is the constant (wedge inclination) and s_0 is the effective spacing of adsorbate molecules at no stress. In the third dimension, the width is considered to be also s_0. The adsorbate molecules are mobile and at the wide end (or mouth) of the pore they communicate with an atmosphere of relative vapor pressure h in the macropores.

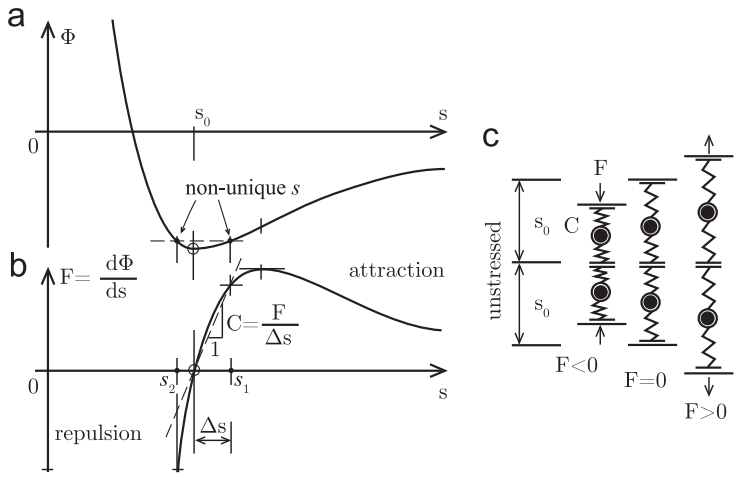

Fig. 2. (a) Interatomic pair potential; (b) the corresponding interatomic force and secant stiffness; and (c) interatomic forces between opposite pore walls visualized by springs.

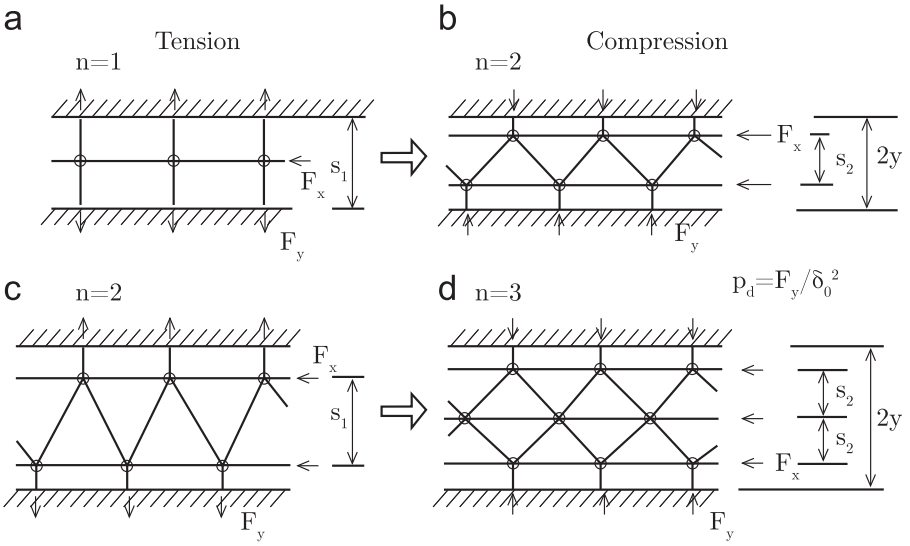

Fig. 3. Various simple idealized molecular arrangements between the walls of a nanopore.

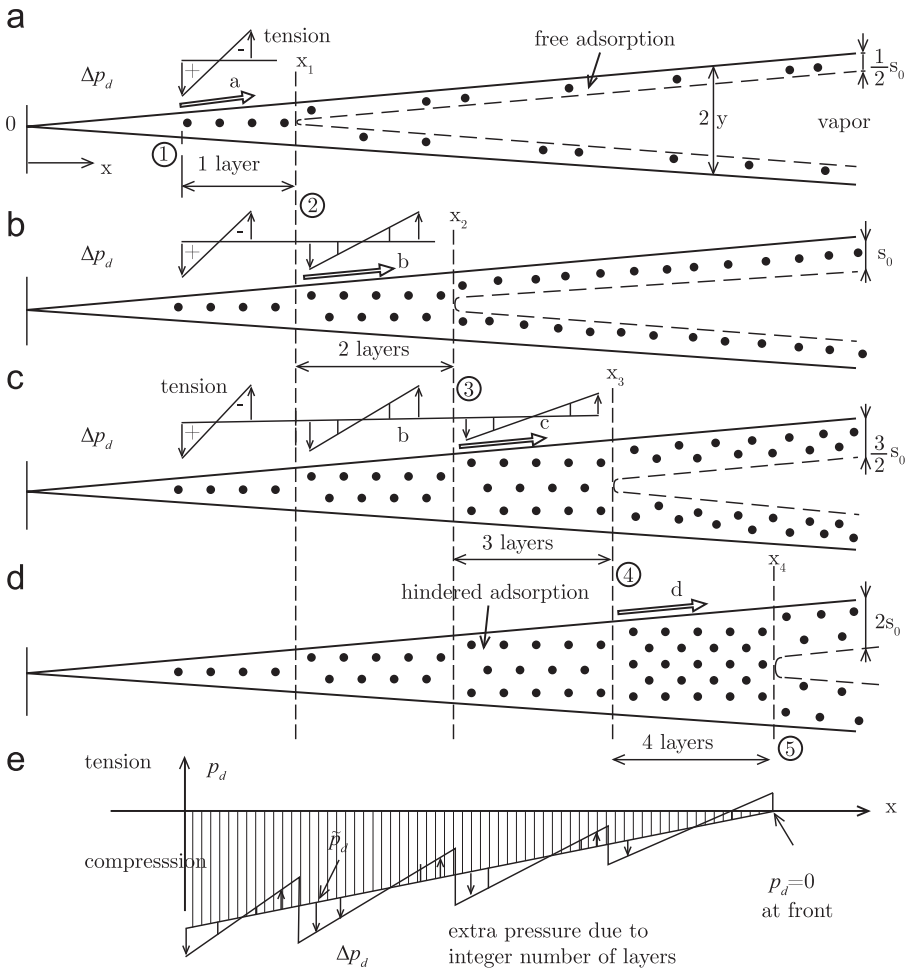

Fig. 4. Filling of a continuously diverging nanopore and disjoining pressures.

We assume the hindered adsorbed layer to be in thermodynamic equilibrium with the vapor in an adjacent macropore. This requires equality of the chemical potentials $\overline{\mu}$ *per molecule* ($\overline{\mu}=\mu/M$, the overbar being used to label a quantity per molecule). At the front of the portion of the nanopore filled by adsorbate, henceforth called the 'filling front' (marked by circled 2, 3 or 4 in Fig. 4), Eq. (10) of continuum thermodynamics gives a zero transverse pressure, $\tilde{p}_d=0$, and so $\overline{\mu}=\overline{\mu}_a=\overline{\mu}_v$.

However, in the discrete treatment of individual molecules, the chemical potential can be altered by transverse tension or compression Δp_d (Fig. 4), which can develop at the filling front and act across the monomolecular layers unless the nanopore width $2y$ at the filling front happens to be an integer multiple of the unstrained molecular spacing s_0. We will call Δp_d the 'misfit' (part of) disjoining (or transverse) pressure, by analogy with the misfit strain energy for a dislocation core in the Peierls–Nabarro model (Hirth and Lothe, 1992).

The misfit pressure, which, at the filling front, represents the total transverse pressure (or stress), is determined by the average change Δs of spacing s between adjacent monomolecular layers, which is

$$\Delta s=2kx/n-s_0 \quad (n=1,2,3,\ldots) \tag{11}$$

where n is the number of monomolecular layers across the nanopore width and s_0 is the natural spacing between the adjacent monomolecular layers in free adsorption, i.e., when the transverse stress vanishes (note that for the triangular arrangements in Fig. 2b and c, s_0 is obviously less than the natural spacing of unstressed adsorbate molecules, shown as s_0 in Fig. 2a). So, the force between the molecules of the adjacent layers is $F=C\Delta s$ and the strain energy of the imagined springs connecting the molecules is $F\Delta s/2$ or $C(\Delta s)^2/2$ per molecule (if, for simplicity, a loading along the secant is considered).

The hindered adsorbed layer is in a multiaxial stress state, for which the total strain energy is the sum of the strain energies of the strain components. Since continuum thermodynamics gives zero disjoining (transverse) pressure p_d at the filling front, it suffices to add to $C_n(\Delta s)^2/2$ the chemical potential $\overline{\mu}_a$ per molecule at the filling front due to longitudinal pressure p_a only. So, in view of Eq. (10), the chemical potential per molecule at the filling front x_n^f with n monomolecular

layers is

$$\overline{\mu}_{f,n}=\frac{C_n}{2}\left(\frac{2kx_f}{n}-s_0\right)^2+\overline{\mu}_a \tag{12}$$

where again the overbar is a label for the quantities per molecule. Since $\tilde{p}_d=0$ at the filling front x^*, the only source of $\overline{\mu}_n$ is the longitudinal spreading pressure p_a in the adsorption layer.

Let us now check whether at some filling front coordinate x^* (Fig. 4) the diverging nanopore is able to contain either n or $n+1$ monomolecular layers with the same chemical potential per molecule. For $n+1$ layers

$$\overline{\mu}_{f,n+1}=\frac{C_n}{2}\left(\frac{2kx}{n+1}-s_0\right)^2+\overline{\mu}_a \tag{13}$$

Setting $\overline{\mu}_n=\overline{\mu}_{n+1}$, we may solve for x. This yields the critical coordinate and critical pore width for which the molecules in n and $n+1$ monomolecular layers have the same chemical potential per molecule:

$$x^*_{f,n}=\frac{\sqrt{C_n}+\sqrt{C_{n+1}}}{\frac{1}{n}\sqrt{C_n}+\frac{1}{n+1}\sqrt{C_{n+1}}}\frac{s_0}{2k},\quad y^*_{f,n}=2kx^*_{f,n} \tag{14}$$

So, the critical relative pore width $2y^*_f/s_0$ at the filling front is a weighted harmonic mean of n and $n+1$ (and a simple harmonic mean if $C_n=C_{n+1}$).

Equality of the chemical potentials per molecule at the filling front for n and $n+1$ monomolecular layers in the same nanopore, which occurs for the pore width given by Eq. (14), implies that no energy needs to be supplied and none to be withdrawn when the number of monomolecular layers is changed between n and $n+1$. So, the equilibrium content of hindered adsorbate in the nanopore for a given chemical potential of vapor is non-unique. Similar to non-uniqueness of capillary surfaces, this non-uniqueness underlies the sorption–desorption hysteresis in the nanopores.

The possibility of non-uniqueness is evident from Fig. 2. For the same value of potential Φ, there are two states with different molecular separations s_1 and s_2, one corresponding to attraction (tension) and one to repulsion (compression), as seen on the horizontal line intersecting the curve of Φ in Fig. 2. Note that the secant stiffness for compression must be larger than it is for tension, which is a point neglected, for the sake of simplicity, in the foregoing calculation.

Misfit disjoining pressure: In view of Eq. (12), its value corresponding to $\overline{\mu}_n$ for n monomolecular layers in the nanopore is

$$p_{d,n}=C_n\left(s_0-\frac{2kx^*}{n}\right)+\tilde{p}_d(x_n) \tag{15}$$

where $\tilde{p}_d(x_n)$, based on continuum thermodynamics, is non-zero if $x_n\neq x_{f,n}$. In contrast to stress, the pressure is considered as positive when compressive. Replacing n with $n+1$, we find that the disjoining pressure makes a jump when the number of monomolecular layers in the nanopore changes from n to $n+1$

$$\Delta p_{d,n}=p_{d,n+1}-p_{d,n}=2kx_n\left(\frac{C_n}{n}-\frac{C_{n+1}}{n+1}\right)+s_0(C_{n+1}-C_n) \tag{16}$$

(see Fig. 4). At the filling front, the jump is from transverse tension to compression (Fig. 5c).

Eq. (16) shows that the sudden jumps $\Delta p_{d,n}$ of the misfit pressures from tension to compression diminish with increasing n ($n=1,2,3,\ldots$), as the nanopore is getting wider; see Figs. 4d and 5c. Therefore, the wider the pore is, the less effective the mechanism of snap-through instabilities is. It ceases to operate for pores of width $n>10$, which are wider than the combined maximum thicknesses of two opposite adsorption layers (about 3 nm).

Note that, since the changes Δs of molecular distance are large, the C values depend on F or Δp_d (Fig. 2b). So, Eq. (16) is actually a nonlinear equation for Δp_d and its numerical solution would require iterations. But here we are aiming at conceptual explanation rather than numerical results.

Misfit chemical potentials and their effect on sorption isotherm: The variation of chemical potential at the filling front x_f is shown in Fig. 5d. Since transverse tension at the filling front gives the same chemical potential as transverse compression of equal magnitude, the misfit chemical potential, defined as the part of chemical potential due to p_d at the filling front, varies continuously, provided the pore width varies continuously, too; see Fig. 5d. This is because transverse tension gives the same chemical potential as transverse compression of equal magnitude.

The total chemical potential at the filling front is obtained by adding the chemical potential $\overline{\mu}_a(x_f)$ obtained from continuum thermodynamics, which yields the potential variation in Fig. 5e. Considering the relation of filling front coordinate x_f to the adsorbate mass w shown (in a smoothed form) in Fig. 5b, and the relation $h=e^{(M/RT)\mu_f}$, one can deduce the solid curve in Fig. 5e representing the diagram of equilibrium states of mass content w versus relative vapor pressure h in the macropore.

Why are the segments of the pressure variation in Fig. 5c linear, and why are the segments of the chemical potential variation in Fig. 5d–f parabolic? The reason is that the variation of nanopore width has been idealized as linear (and that the plots are made for constant C). These segments take different shapes for other width variations.

Sequential snap-throughs of adsorbate content: In sorption testing and most practical problems, the relative vapor pressure h is the variable that is controlled, and the adsorbate mass w is the response. Consequently, the states at the

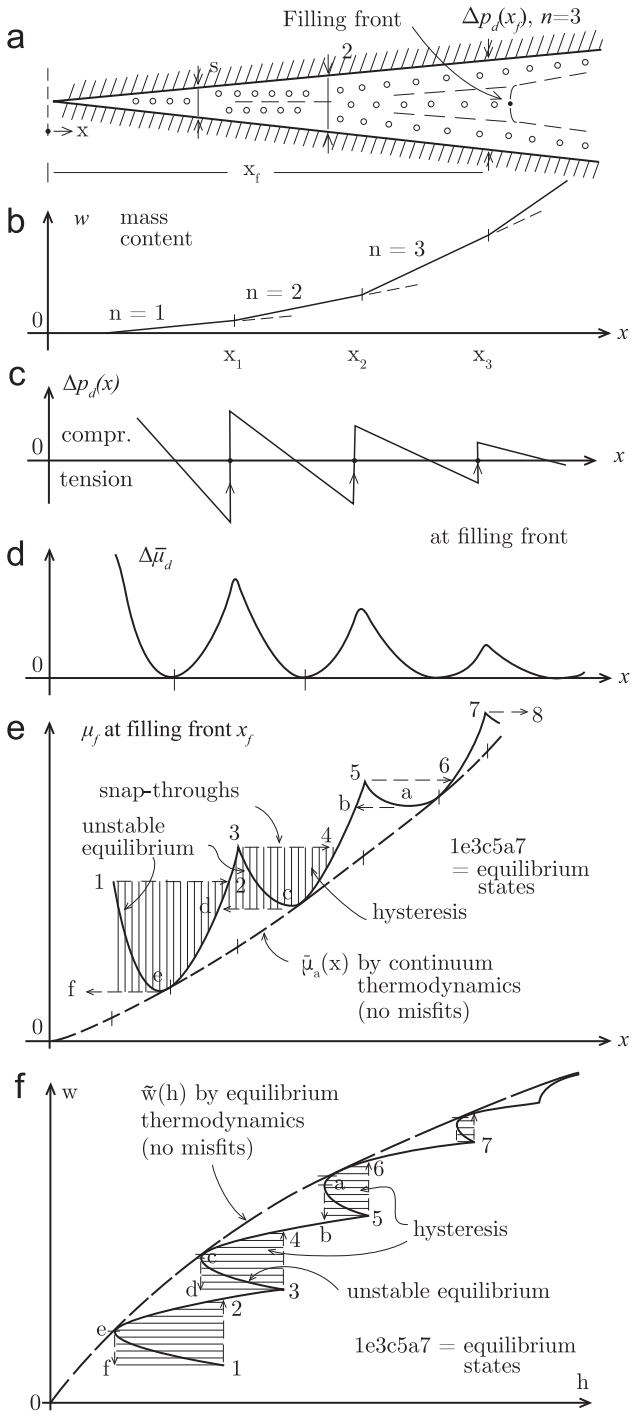

Fig. 5. Misfit disjoining pressures and chemical potentials in a continuously diverging nanopore, with dynamic snap-throughs of adsorbate content.

reversal points 1, 3, 5, 7 of the equilibrium diagram in Fig. 5 for the diverging nanopore are unstable. Likewise, the states at points 1, 3, 5, 7 in Fig. 6d for the nanopore of step-wise variable width. The loss of stability can be evidenced by checking that the molecular potential loses positive definiteness. Fundamental though such checks may be, it is simpler and more intuitive to argue in terms of infinitely small deviations dh from the equilibrium state.

Consider, e.g., that, in Fig. 5f or 6d, a sufficiently slow gradual increase of h has moved the equilibrium state from point 2 to point 3, which is a local maximum of h as a function of w. For a further infinitesimal increase dh, there is on the equilibrium diagram no longer any point close to point 3. So, borrowing a term from structural mechanics (Bažant and Cedolin, 1991), we realize that the adsorbate mass content w must dynamically 'snap through' at constant h along vertical line 34 to point 4. After dissipating the energy released along segment 34 (the rate of which depends on the lingering times of adsorbed molecules and diffusion along the hindered adsorbed layer; Bažant and Moschovidis, 1973), thermodynamic

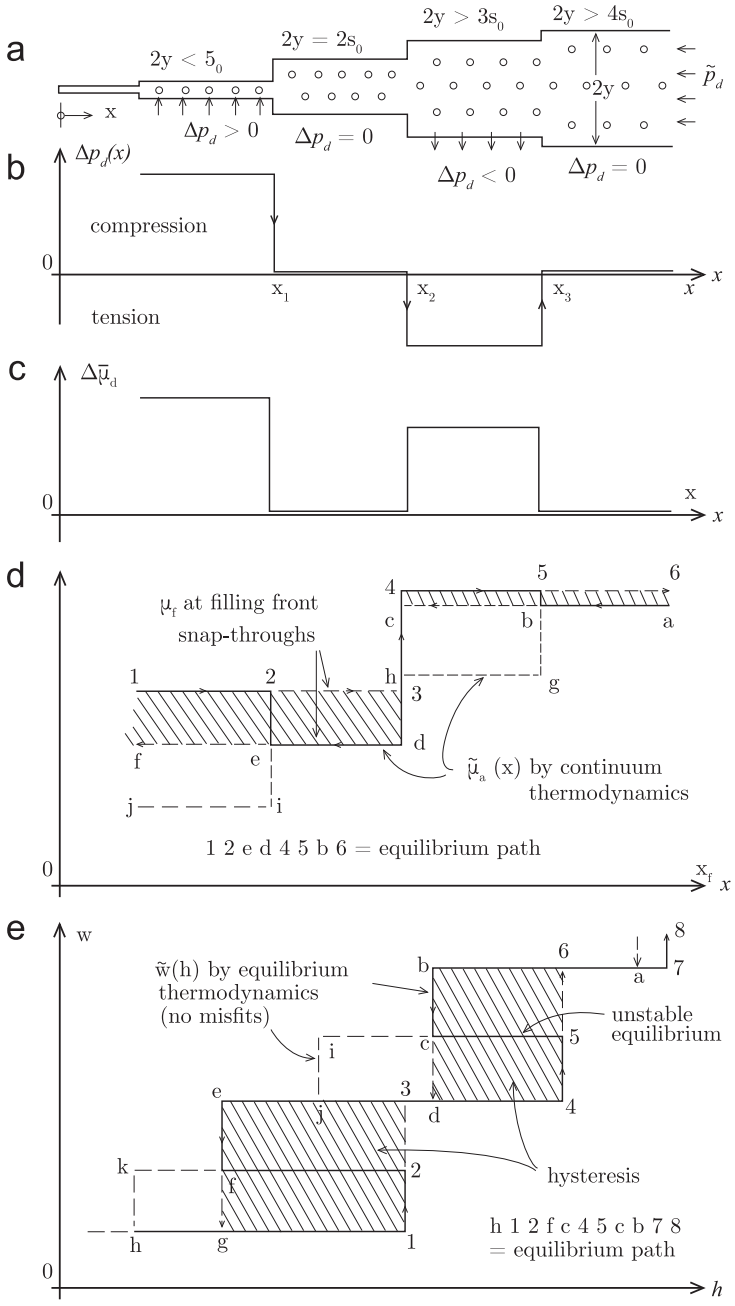

Fig. 6. Step-wise diverging nanopore and misfit disjoining pressures.

equilibrium is recovered at point 4. It is stable because a further infinitesimal increment of dh finds, next to point 4, an equilibrium state with adsorbate content incremented by dw.

If h is increased slowly enough further, the equilibrium system will move from point 4 to point 5 at which a local maximum of h is reached again and the loss of stability gets repeated, since a further increase dh can find equilibrium only after a dynamic snap-through to point 6. Each snap-through will release some energy which must be damped and dissipated by the system. So, the local maxima of h at points 1, 3, 5 and 7 are the critical states giving rise to the so-called 'snap-through instability' (Bažant and Cedolin, 1991). The equilibrium states on curved segments 1e2, 3c4 and 5a6 are unstable and can never be reached in reality.

The salient feature is that a different path $w(h)$ is followed when h is decreased. To show it, consider point 7 in Fig. 5f or 6d as the starting point. During a slow enough decrease h, the system will follow the stable states along segment 76a until a local minimum of h is reached at point a, which is the stability limit. Indeed, if h is further decremented by dh, there is no equilibrium state near point a. So, the equilibrium state a is unstable and the system will 'snap through' dynamically at constant h along path ab. At point b stable equilibrium is regained after sufficient time. When h is decreased further slowly enough, the equilibrium states move through segment b4c until again a local minimum of h is reached and stability is lost at point c. Thereafter, the system 'snaps through' along line cd to point d, where equilibrium is regained, etc.

In the diverging pore in Fig. 5, the snap-through means that when the equilibrium filling front reaches the critical points, x_1,x_2, or x_3, it will advance forward a certain distance at constant h, as fast as diffusion along the micropore, controlled by the lingering times of the adsorbate molecules, will permit.

The cross-hatched areas in between the sorption and desorption isotherms, such as area 34*cd*3 in Fig. 5e or 6d, represent sorption hysteresis. They also characterize energy dissipation.

Sequential snap-throughs for step-wise nanopore width variation: The diagrams in Fig. 5d–f are valid only for a micropore with continuously diverging rigid planar walls (Fig. 5a). This is, of course, an idealization. Because of the atomistic structure of pore walls, the pore width in reality varies discontinuously, as exemplified in Fig. 6a. The chance of a width exactly equal to an integer multiple of s_0 is small.

Consider that the jumps of nanopore width (Fig. 6a) occur at x_1,x_2,x_3, . . ., and that at x_1 is narrower than s_0, at x_2 exactly equal to $2s_0$, and at x_3 wider than $3s_0$. Thus, the filling front in pore segment (x_1,x_2) is in transverse compression, in segment (x_2,x_3) at zero transverse pressure, and in segment (x_3,x_4) in transverse tension; see Fig. 6b. The corresponding strain energies, representing the misfit chemical potential $\Delta\overline{\mu}_d$ per molecule, have a pulse-like variation as shown in Fig. 6c. Continuum thermodynamics, which ignores the misfits, gives a monotonically rising staircase variation of the chemical potential $\tilde{\mu}_a(x)$ (per unit mass) as a function of the filling front coordinate x_f, represented by path *jiedhgba* (Fig. 6d). Superposing on this staircase the misfit chemical potential $\Delta\overline{\mu}_d$ (converted to unit mass), one gets the non-monotonic step-wise path of equilibrium states, shown by the bold line 12ed455b6 in Fig. 6d.

Taking into account the dependence of the adsorbate mass w in the nanopore on the filling front coordinate x_f, one can covert the diagram in Fig. 6d into the sorption isotherm in Fig. 6e, usually plotted as w versus h. The monotonic staircase *hkfejicba* would represent the equilibrium path if the misfit disjoining pressures were ignored.

When the rise of h, and thus μ_f, is controlled, the segments 23 and 56 in Fig. 6e are unstable and unreachable. Indeed, when h or μ_f is infinitesimally increased above point 2, there is no nearby equilibrium state, and so the system will 'snap through' dynamically to point 3. At that point, equilibrium is regained, and h and μ_f can be raised again, slowly enough to maintain equilibrium, along path 345. A similar dynamic snap-through is repeated along segment 56, after which the stable segment 678 can be followed. Likewise, in the diagram of μ_f versus the filling front coordinate x_f (Fig. 6d), forward snap-throughs at increasing μ_f (which is a monotonically increasing function of h) occur along segments 23 and 56.

When h or μ_f is decreased slowly enough from point 8, the stable equilibrium path 876*bc* is followed until stability is lost at point *c* (Fig. 6e). Then, the system snaps through dynamically from *c* to *d*, follows equilibrium path *def*, and snaps dynamically from *f* to *g*. Likewise, in Fig. 6d, backward snap-throughs at decreasing μ_f occur along segments *bc* and *ef*.

Obviously, the states on segments *c*5 and *f*2 in Fig. 6e, or 2*e* and 5*e* in Fig. 6d, can never be reached. They represent unstable equilibrium. The shaded areas *g*13*eg* and *d*46*bd* represent hysteresis, which leads to energy dissipation.

Snap-throughs in a system of nanopores: The diverging nanopore (Figs. 4, 5a and 6a) is not the only pore geometry producing sorption hysteresis. There are infinitely many such geometries. In the simple model of discrete monolayers pursued in Part I, the only geometry avoiding hysteresis due to sequential snap-throughs is hypothetical—the widths of all the nanopores would have to be exactly equal to the integer multiples of the natural spacing s_0 of monomolecular layers in free adsorption, so as to annul the misfit pressures. Below, we will show that if molecular coalescence is allowed in the lateral direction, then even these special pore geometries will exhibit sorption hysteresis, and so the effect is extremely general.

An essential feature of nanoporosity is that there are nanopores of many different thicknesses $2y$ densely distributed as shown in Fig. 7. At a given vapor pressure, all the nanopores that are narrower than a certain width $2y$ are filled by adsorbed water and the wider ones are empty, containing only vapor; see Fig. 7a, c and e.

As the relative pore pressure h is increased, larger and larger pores fill up. A critical state (or a local maximum of h) is reached for a pore width at which the misfit chemical potential $\Delta\mu_d$ due to misfit disjoining pressure is for n monomolecular layers equal to or larger than the misfit chemical potential for $n+1$ layers. After that state, the system loses stability and regains it only when all the nanopores up to a certain larger width get filled without increasing h. For decreasing h, the stability loss would occur for a different pore width.

The distribution of nanopore thicknesses $2y$ may be characterized by a continuous cumulative frequency distribution function $\varphi(y)$ that represents the combined volume of all the nanopores with thicknesses $<2y$. This case, though, is not qualitatively different from the diverging nanopore studied previously. For $\varphi(y)\propto ky^2$, the nanopore system in Fig. 7 becomes mathematically equivalent to the linearly diverging nanopore studied before.

The way the hysteresis in the individual nanopores gets superposed to produce a pronounced hysteresis on the macroscale is schematically illustrated in Fig. 8.

Rough or non-matching nanopore surfaces: For hydrated cement, a smooth pore surface is surely an idealization, needed to render the calculations simple. In reality, the pore surface is irregular, random and rough. Recently, it has been shown (Yang et al., 2011) by MD simulations of nitrogen in carbon slit-pores that random surface roughness of approximately the same amplitude as the fluid molecule diameter effectively damps the oscillations of the disjoining pressure, compared to molecularly smooth surfaces. However, it is doubtful that this is true locally, for the disjoining intermolecular forces individually. The preceding observations regarding a system of nanopores applies to arbitrarily short nanopores, and a rough pore can be imagined as a series of very short smooth nanopores. The roughness aspect calls for deeper study.

Even if the nanopore surface is a regular atomic lattice, the spacing of surface atoms generally does not match the equilibrium spacing of adsorbate molecules along the pore. This imposes a wavy potential of transverse intermolecular forces with non-matching wavelength. This potential will alter the locations of the snap-throughs.

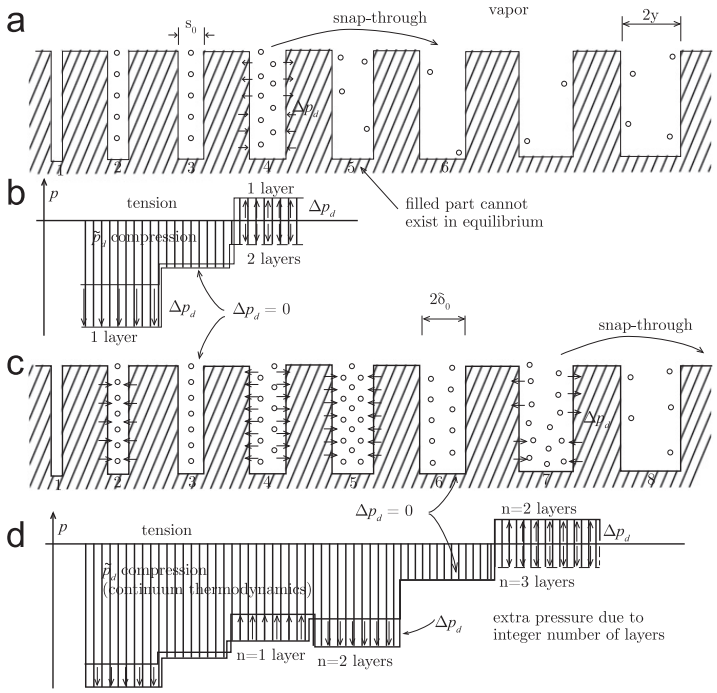

Fig. 7. System of nanopores of different widths communicating through vapor phase.

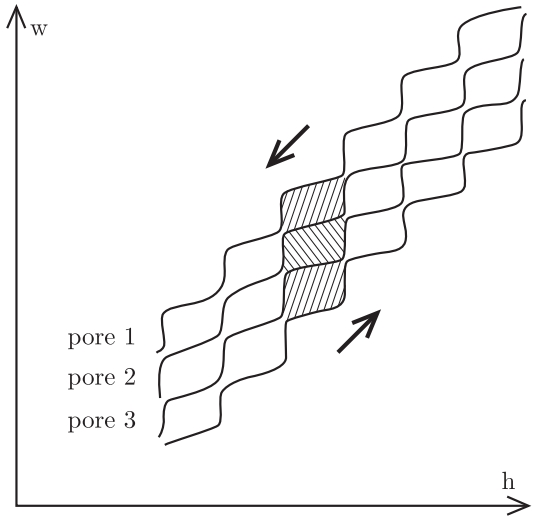

Fig. 8. Superposition of hysteretic loops from different nanopores.

Temperature: The present analysis of snap throughs focuses on isolated, fixed molecular energy barriers and thus neglects some important thermal effects in the adsorbate. Temperature appears in the present analysis via the entropy of the vapor phase (which defines the humidity) and the reversible, continuum isotherm for multi-layer adsorption. The free energy barriers for snap through instabilities are related to discrete molecular inclined forces without accounting for entropic contributions and molecular rearrangements that constantly vary the barrier energy and structure. At low temperatures, this solid-like picture of the adsorbate with long-lived molecular states is valid, and snap throughs can occur by rare, thermally activated transitions over the energy barriers related to inclined molecular forces in non-uniform pore geometries.

This model, however, neglects the balance between the same attractive lateral interactions and the entropy of discrete molecular rearrangements on the surface, which can lead to 'phase separation' into low-density and high-density phases in the adsorbate (Gelb et al., 1999). Such effects dominate at low temperature (below the 'critical hysteresis temperature') and can lead to sorption hysteresis even in perfectly straight nanopores. Variations in the nanopore geometry, however, do provide additional free energy barriers for molecular condensation and snap throughs between different pore regions. As shown in Part II, these temperature-dependent phenomena can be treated using non-equilibrium statistical thermodynamics, which provides a general theory of molecular condensation in nanoporous solids building on this work.

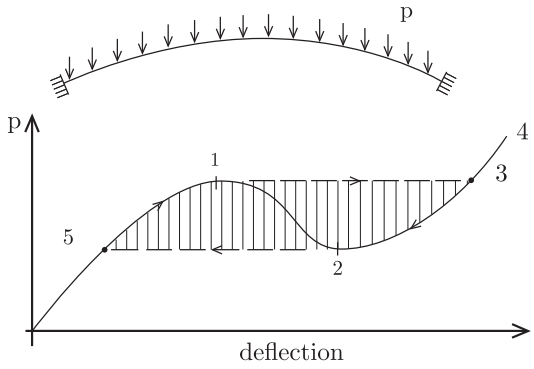

Fig. 9. Analogy with snap-through of an arch.

Analogy with snap-through buckling of flat arch: There is an instructive analogy with the snap-through buckling of elastic arches or shells under controlled load (Bažant and Cedolin, 1991, Fig. 9, p. 231). If the arch is flat enough and flexible enough not to fracture, the equilibrium diagram of total load p versus midspan deflection u follows the diagram sketched in Fig. 9. The segments 051 and 432 consist of stable states at which the potential energy is positive definite (i.e., has a strict local minimum). But this is not true for the equilibrium states on the segment 12, at which the potential energy does not have a strict local minimum.

Consider that load p is increased from point 0 up to the local maximum at critical point 1 (Fig. 9). If load p is increased further by an infinitesimal amount ddp, there is no nearby equilibrium state. The arch must follow at constant load the dynamic snap-through path 14, during which there is accelerated motion. The load difference from the equilibrium curve below represents the inertial force, which provides rightward acceleration. The arch gains kinetic energy up to point 3, swings over (along a horizontal line), and then vibrates at constant load about point 3 until the kinetic energy is dissipated by damping (without damping, it would vibrate indefinitely). Then, if the load is increased further, the arch moves through stable equilibrium states on the segment 34.

When the load is decreased, starting at point 4, the arch will follow the stable equilibrium states along segment 432 until a local minimum is reached at point 2. If the load is decreased further by an infinitesimal amount $\mathrm{d}P$, there is no equilibrium state near point 2. So, the arch must snap through dynamically to point 5, the load being again balanced by inertia forces which provide leftward acceleration. During this snap-through the arch gains kinetic energy, swings over to the left of point 5 and vibrates about point 5 until the kinetic energy is dissipated by damping. Then, the load can be decreased further following the stable equilibrium states below point 5.

Note that even though the arch is elastic and the structure–load system is conservative, hysteresis is inevitable. During the cycle, the arch dissipates an energy equal to the cross-hatched area 51325 in Fig. 4.

Energy dissipated by hysteresis and material damage: The Gibbs free energy dissipated per unit mass of the nanoporous material is $\mathrm{d}G = w\,\mathrm{d}\mu$, where $\mathrm{d}\mu = RT/M\,\mathrm{d}\ln h$, which has in thermodynamic equilibrium the value for the adsorbate species in the vapor and for the adsorbed phases. Therefore, the free energy dissipated per unit volume of material due to the hysteresis during a complete cycle, e.g., a drying–wetting cycle of hardened cement paste, is

$$\Delta G = \frac{RT}{M}\oint \frac{w(h)}{h}\,\mathrm{d}h \tag{17}$$

Since h is in the denominator, integrability, i.e., the finiteness of ΔG, requires that $\lim_{h\to 0} w/h = 1/h^n$, where $0 \le n < 1$. Graphically, ΔG is proportional to the area between the sorption and desorption isotherms in the diagram of w/h versus h (Fig. 10).

The energy could be dissipated in two ways:

(1) By internal friction in the adsorbed fluid during the dynamic snap-throughs (or the molecular coalescence phenomena discussed in Part II Bazant and Bažant) or
(2) by fracturing or plastic damage to the nanopore surfaces.

However, the latter seems unlikely since it could be associated with every disjoining pressure change and not particularly with the snap-through. The existence of the former is undeniable, and the point here is to show that the hysteresis is perfectly explicable without postulating any damage to the nanopore surface.

Anyway, the degree of material damage due to a drying–wetting cycle, if any, could be checked by measuring the strength or the fracture energy, or both, of the material before and after the cycle. This would have to be done slowly enough on thin enough specimens having drying half-times less than 1 h (<1 mm thick for cement paste), in which the relative humidity h in the capillary pores can be changed without creating a significant gradient of h across the specimen wall (in thicker samples, most of the material damage is done by non-uniform shrinkage stresses engendered by non-uniformity of h across the wall thickness Bažant and Raftshol, 1982). Shrinkage and creep experiments on such specimens

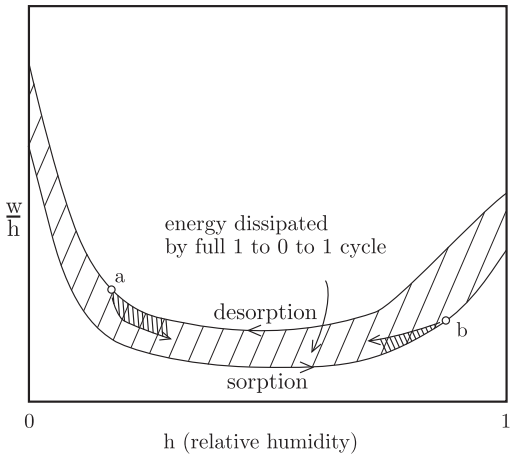

Fig. 10. Energy dissipated by sorption hysteresis on a full h-cycle $1\to0\to1$ (shaded area), and dissipation during mid-range reversals (a, b).

have been performed at Northwestern (Bažant et al., 1976), but no cycles were performed and strength changes were not checked. It could also be checked whether the snap-throughs might be associated with the acceleration of concrete creep due to simultaneous drying, called the drying creep (or the Pickett effect).

Sorption potential: Note that, based on the derivation of Eq. (17), it further follows that

$$\beta = \frac{RT}{M}\frac{w}{h} = \frac{\partial G}{\partial h} \tag{18}$$

In other words, Gibbs's free energy per unit mass of adsorbate as a function of h is a potential for the adsorbate content parameter β during a one-way change of h.

Is the atomic crystal structure of pore walls relevant? The spacing of atoms in the pore walls imposes on the attractive potential a waviness whose wavelength generally differs from the in-plane spacing of the adsorbate molecules. However, it would be incorrect to consider the adsorbate molecule to jump over the peaks of this wavy attractive potential. The reason is that such jumps are not rare hopping processes. Unlike solids, the adsorbate molecules undergo constant vigorous rearrangements (except during solidification at extremely low temperature). Thus, they feel only the average surface properties and have strong entropic/steric interactions with the surface. In liquids and gases, the entropy prevails over bond enthalpy and prevents long-lived solid-like states connected by thermal hopping.

4. Conclusions of Part I

We can summarize the findings of the first part as follows:

1. One mechanism that must be causing sorption hysteresis at low vapor pressure is a series of snap-through instabilities causing path-dependent non-uniqueness of adsorbate content and dynamic jumps of water content of nanopores at constant vapor pressure.
2. The snap-through instabilities are a consequence of the discreteness of the adsorbate, which leads to non-uniqueness of mass content and to misfit disjoining (transverse) pressures due to a difference between the pore width and an integer multiple of the thickness of a transversely unstressed monomolecular layer of the adsorbate.
3. The hysteresis is explained by the fact that the snap-through instabilities for sorption and desorption follow different paths.
4. The wider the pore, the weaker the mechanism of snap-through instabilities. This mechanism cannot operate in pores wider than about 3 nm.
5. The snap-through instabilities are analogous to snap-through buckling of arches and shells, long known in structural mechanics. They cause hysteresis and energy dissipation even when the arch or shell is perfectly elastic and the load conservative.

If a quantitative version of this theory were developed, it might be possible to infer from the hysteresis the surface area and the size distribution of the nanopores filled by hindered adsorbate. Our preliminary analysis of snap-through instabilities suggests that the key to making this connection is to also account for inclined forces and 'lateral interactions', in the statistical thermodynamics of hindered adsorption. Part II will show that attractive lateral interactions generally lead to sorption hysteresis in any pore geometry due to molecular coalescence of the adsorbate (Bazant and Bažant).

Acknowledgment

The research was funded partly by the U.S. National Science Foundation under Grant CMS-0556323 to Northwestern University (ZPB) and Grant DMS-0948071 to MIT (MZB) and partly by the U.S. Department of Transportation under Grant 27323 provided through the Infrastructure Technology Institute of Northwestern University (ZPB). Thanks are due to Franz-Josef Ulm and Rolland J.-M. Pellenq of MIT for stimulating discussions of disjoining pressure based on MD simulations, and to Laurent Brochard and Hamlin M. Jennings for further valuable discourse.

References

Adolphs, J., Setzer, M.J., 1996. A model to describe adsorption isotherms. J. Colloid Interface Sci. 180, 70–76.
Adolphs, J., Setzer, M.J., Heine, P., 2002. Changes in pore structure and mercury contact angle of hardened cement paste depending on relative humidity. Mater. Struct. 35, 477–486.
Balbuena, P.B., Berry, D., Gubbins, K.E., 1993. Solvation pressures for simple fluids in micropores. J. Phys. Chem. 97, 937–943.
Baroghel-Bouny, V., 2007. Water vapour sorption experiments on hardened cementitious materials. Part I: essential tool for analysis of hygral behaviour and its relation to pore structure. Cem. Concr. Res. 37, 414–437.
Bažant, Z.P., 1970a. Constitutive equation for concrete creep and shrinkage based on thermodynamics of multi-phase systems. Mater. Struct. 3, 3–36. (reprinted in Wittmann, F.H. (Ed.), Fifty Years of Evolution of Science and Technology of Building Materials and Structures, RILEM, Aedificatio Publishers, Freiburg, Germany, 1997, pp. 377–410).
Bažant, Z.P., 1970b. Delayed thermal dilatations of cement paste and concrete due to mass transport. Nucl. Eng. Des. 24, 308–318.
Bažant, Z.P., 1972a. Thermodynamics of interacting continua with surfaces and creep analysis of concrete structures. Nucl. Eng. Des. 20, 477–505.
Bažant, Z.P., 1972b. Thermodynamics of hindered adsorption with application to cement paste and concrete. Cem. Concr. Res. 2, 1–16.
Bažant, Z.P., 1975. Theory of creep and shrinkage in concrete structures: a précis of recent developments. In: Nemat-Nasser, S. (Ed.), Mechanics Today (Am. Acad. Mech.), vol. 2. Pergamon Press, pp. 1–93.
Bažant, Z.P., Asghari, A.A., Schmidt, J., 1976. Experimental study of creep of hardened cement paste at variable water content. Mater. Struct. (RILEM, Paris) 9, 190–279.
Bažant, Z.P., Cedolin, L., 1991. Stability of Structures: Elastic, Inelastic, Fracture and Damage Theories. Oxford University Press, New York (2nd ed. Dover Publications, 2003; 3rd ed. World Scientific Publishing, Singapore, NJ, London, 2010).
Bažant, Z.P., Kaplan, M.F., 1996. Concrete at High Temperatures: Material Properties and Mathematical Models. Longman (Addison-Wesley), London (2nd ed. Pearson Education, Edinburgh, 2002).
Bažant, Z.P., Moschovidis, Z., 1973. Surface diffusion theory for the drying creep effect in Portland cement paste and concrete. J. Am. Ceram. Soc. 56, 235–241.
Bažant, Z.P., Raftshol, W.J., 1982. Effect of cracking in drying and shrinkage specimens. Cem. Concr. Res. 12, 209–226. Disc. 797–798.
Bažant, Z.P., Thonguthai, W., 1978. Pore pressure and drying of concrete at high temperature. Proc. ASCE, J. Eng. Mech. Div. 104, 1058–1080.
Bazant, M.Z., Bažant, Z.P. Theory of sorption hysteresis in nanoporous solids: II. Molecular coalescence, J. Mech. Phys. Solids, http://dx.doi.org/10.1016/j.jmps.2012.04.015, this issue.
Bonnaud, P.A., Coasne, B., Pellenq, R.J.-M., 2010. Molecular simulation of water confined in nanoporous silica. J. Phys.: Condens. Matter, 284110. (15pp.).
Brochard, L., Vandamme, M., Pellenq, R.J.-M., Teddy, F.-C., 2011. Adsorption-induced deformation of microporous materials: coal swelling induced by CO_2?CH_4 competitive adsorption langmuir, 28 (5), 2659–2670. Publication Date (Web): December 20, 2011 (Article) http://dx.doi.org/10.1021/la204072d.
Brochard, L., Vandamme, M., Pellenq, R.J.-M., 2012. Poromechanics of microporous media. J. Mech. Phys. Solids 60 (4), 606–622. http://dx.doi.org/10.1016/j.jmps.2012.01.001.
Brunauer, S., 1943. The Adsorption of Gases and Vapors. Princeton University Press, Princeton, NJ, p. 398.
Brunauer, S., Emmett, P.T., Teller, E., 1938. Adsorption of gases in multi-molecular layers. J. Am. Chem. Soc. 60, 309–319.
Cerofolini, G.F., Meda, L., 1998a. A theory of multilayer adsorption on rough surfaces in terms of clustering and melting BET piles. Surf. Sci. 416, 402–432.
Cerofolini, G.F., Meda, L., 1998b. Clustering and melting in multilayer equilibrium adsorption. J. Colloid Interface Sci. 202, 104–123.
Coasne, B., Galarneau, A., Di Renzo, F., Pellenq, R.J.-M., 2008a. Molecular simulation of adsorption and intrusion in nanopores. Adsorption 14, 215–221.
Coasne, B., Di Renzo, F., Galarneau, A., Pellenq, R.J.-M., 2008b. Adsorption of simple fluid on silica surface and nanopore: effect of surface chemistry and pore shape. Langmuir 24, 7285–7293.
Coasne, B., Galarneau, A., Di Renzo, F., Pellenq, R.J.-M., 2009. Intrusion and retraction of fluids in nanopores: effect of morphological heterogeneity. J. Phys. Chem. C 113, 1953–1962.
Derjaguin, B.V., 1940. On the repulsive forces between charged colloid particles and the theory of slow coagulation and stability of lyophile sols. Trans. Faraday Soc. 36, 203. 730.
Espinosa, R.M., Franke, L., 2006. Influence of the age and drying process on pore structure and sorption isotherms of hardened cement paste. Cem. Concr. Res. 36, 1969–1984. (Figs. 2, 6, 16).
Feldman, R.F., Sereda, P.J., 1964. Sorption of water on compacts of bottle hydrated cement. I: the sorption and length-change isotherms. J. Appl. Chem. 14, 87.
Feldman, R.F., Sereda, P.J., 1968. A model for hydrated Portland cement paste as deduced from sorption-length change and mechanical properties. Mater. Struct. 1 (6), 509–520.
Gelb, L.D., Gubbins, K.E., Radhakrishnan, R., Sliwinska-Bartkowiak, M., 1999. Phase separation in confined systems. Rep. Prog. Phys. 62, 1573–1659.
Hall, C., Hoff, D., Taylor, S.C., Wilson, M.A., Yoon, B.G., Reinhardt, H.-W., Sossoro, M., Meredith, P., Donald, A.M., 1995. Water anomaly in capillary liquid absorption by cement-based materials. J. Mater. Sci. Lett. 14, 1178–1181.
Hirth, J.P., Lothe, J., 1992. Theory of Dislocations. Kreiger.
Jennings, H.M., 2000. A model for the microstructure of calcium silicate hydrate in cement paste. Cem. Concr. Res. 30, 101–116.
Jennings, H.M. Pores and viscoelastic properties of cement paste, submitted for publication.
Jennings, H.M., Bullard, J.W., Thomas, J.J., Andrade, J.E., Chen, J.J., Scherer, G.W., 2008. Characterization and modeling of pores and surfaces in cement paste: correlations to processing and properties. J. Adv. Concr. Technol. 6 (1), 5–29.
Jönson, B., Wennerström, H., Nonat, A., Cabane, B., 2004. Onset of cohesion in cement paste. Langmuir 20, 6702–6709.
Jönson, B., Nonat, A., Labbez, C., Cabane, B., Wennerström, H., 2005. Controlling the cohesion of cement paste. Langmuir 21, 9211–9221.
Malani, A., Ayappa, K.G., Murad, S., 2009. Influence of hydrophillic surface specificity on the structural properties of confined water. J. Phys. Chem. 113, 13825–13839.
Nikitas, P., 1996. A simple statistical mechanical approach for studying multilayer adsorption: extensions of the BET adsorption isotherm. J. Phys. Chem. 100, 15247–15254.
Pellenq, R.J.-M., Kushima, A., Shashavari, R., Van Vliet, K.J., Buehler, M.J., Yip, S., Ulm, F.-J., 2010. A realistic molecular model of cement hydrates. Proc. Nat. Acad. Sci. 106 (38), 16102–17107.
Powers, T.C., 1965. Mechanism of shrinkage and reversible creep of hardened cement paste. In: International Conference on the Structure of Concrete, Imperial College, London, Paper G1. Cement & Concrete Association, UK.

Powers, T.C., 1966. Some observations on the interpretation of creep data. Bull. RILEM (Paris), 381.
Powers, T.C., Brownyard, T.L., 1946. Studies of the physical properties of hardened portland cement paste. Part 2. Studies of water fixation. J. Am. Concr. Inst. 18 (3), 249–336.
Rarick, R.L., Bhatty, J.W., Jennings, H.M., 1995. Surface area measurement using gas sorption: application to cement paste. In: Skalny, J., Mindess, S. (Eds.), Material Science of Concrete IV, American Ceramic Society, pp. 1–41. (Chapter 1).
Scherer, G.W., 1999. Structure and properties of gels. Cem. Concr. Res. 29, 1149–1157.
Smith, D.E., Wang, Y., Chaturvedi, A., Whitley, H.D., 2006. Molecular simulations of the pressure, temperature, and chemical potential dependencies of clay swelling. J. Phys. Chem. B 110, 20046–20054.
Thomas, J.J., Allen, A.J., Jennings, H.M., 2008. Structural changes to the calcium hydrate gel phase of hydrated cement with age, drying and resaturation. J. Am. Ceram. Soc. 91 (10), 3362–3369.
Vandamme, M., Brochard, L., Lecampion, B., Coussy, O., 2010. Adsorption and strain: the CO_2-induced swelling of coal. J. Mech. Phys. Solids 58, 1489–1505.
Yang, K., Lin, Y., Lu, X., Neimark, A.V., 2011. Solvation forces between molecularly rough surfaces. J. Colloid Interface Sci. 362, 382–388.